Limnol. Oceanogr., 53(6), 2008, 2655–2667
© 2008, by the American Society of Limnology and Oceanography, Inc.

Tracing abyssal food supply back to upper-ocean processes over a 17-year time series in the northeast Pacific

K. L. Smith, Jr. and H. A. Ruhl
Monterey Bay Aquarium Research Institute, 7700 Sandholdt Road, Moss Landing, California 95039

R. S. Kaufmann
Marine Science and Environmental Studies Department, University of San Diego, 5998 Alcalá Park, San Diego, California 92110

M. Kahru
Integrative Oceanography Division, Scripps Institution of Oceanography, University of California, San Diego, 9500 Gilman Drive, La Jolla, California 92093-0218

Abstract

Detrital aggregates episodically deposited on the seafloor represent an underestimated food source to deep-sea communities. A 17-yr time-series study was conducted from 1990 to 2006 in the abyssal northeast Pacific (Sta. M, 4100 m in depth) to evaluate the importance of this food source and its temporal relationship to water column and surface ocean processes. Detrital aggregates appeared on the seafloor from June through December, with the highest peaks in 1990, 1994, 2001, and 2002 reaching a maximum density of 23 m^{-2} in fall 2001. A total of 15,816 aggregates were measured, most less than 20 cm^2 in area and with a mode of 9 cm^2. Density of detrital aggregates was highly correlated with particulate organic carbon (POC) flux at 600 and 50 m above the bottom ($p < 0.001$) with no time lag. Export flux of organic carbon from the euphotic zone was significantly correlated with aggregate density, lagged earlier by 1–4 months ($p \leq 0.001$). Zooplankton displacement volume was significantly correlated with POC flux ($p = 0.023$) and with detrital aggregate density ($p = 0.028$) on the seafloor when lagged earlier by $\leq$1 month. The Bakun upwelling index computed for the region around Sta. M was significantly correlated with detrital aggregate density when lagged earlier by 2–5 months ($p < 0.001$). A strong correlation exists between surface ocean processes and abyssal food supply, including POC flux and detrital aggregates. This direct coupling through the entire water column must be considered in resolving the marine carbon cycle.

Deep-sea communities are fueled by food produced and packaged in the upper water column. Primary production, the originating source of organic carbon, is influenced by temperature, light, stratification, and nutrient supply, which are intimately linked to climate (Behrenfeld et al. 2006). Warming increases ocean stratification and decreases nutrient supply, favoring smaller phytoplankton and resulting in lower export flux rates than are measured when primary production is dominated by larger organisms, such as diatoms (Bopp et al. 2005). Transfer efficiency of sinking particulate organic carbon (POC) between the euphotic zone and 500 m in depth is substantially less in oceanic areas dominated by smaller plankton (Buesseler et al. 2007). Export flux of photosynthetically derived organic carbon estimated from satellite ocean color and sea surface temperature also has been correlated with abyssal POC flux measured from sedimentation trap collections (Smith et al. 2006). Ultimately, sinking flux either is consumed in the water column or settles to the seafloor, where it provides energy and nutrients for benthic communities. In this study, we examined the settling of sinking particulate matter as detrital aggregates, visually apparent on the seafloor. Previous studies have shown that detrital aggregates are seasonally present on the seafloor in the northeast (NE) Pacific, primarily in the summer and fall (Smith et al. 1994, 1998). The correlation between climate indices, such as the multivariate El Niño Southern Oscillation Index (MEI) and Northern Oscillation Index (NOI), and POC flux at abyssal depths in the NE Pacific prompted an examination of detrital aggregates on the seafloor over a 17-yr time series as a measure of food supply reaching the benthic community.

Acknowledgments

This long time-series study required the support of many scientists, technicians, students, and ships' crews on a large number of ships. We especially thank our colleagues Roberta Baldwin, Fred Uhlman, and Bob Wilson, who were always there throughout this study, guaranteeing the success of the program both at sea and ashore. Jake Ellena and Mike Vardaro contributed to the shipboard program during the later years. We thank the Sea-viewing Wide Field-of-View Sensor (SeaWiFS) Project, the National Aeronautics and Space Administration (NASA) Ocean Biology Processing Group, and the Physical Oceanography Distributed Active Archive Center (PO.DAAC) for satellite data. We greatly appreciate access to the California Current Ecosystem (CCE) Long-Term Ecological Research (LTER) website for the zooplankton displacement volume data, and we thank Mark Ohman for valuable discussions. Stace Beaulieu, two anonymous reviewers, and the editors provided excellent comments that improved the manuscript.

This research was supported by National Science Foundation grants OCE89-22620, OCE92-17334, OCE98-07103, and OCE0242472 to K.L.S. as well as funding from the University of California–San Diego, Scripps Institution of Oceanography, and the David and Lucile Packard Foundation.

Detrital aggregates are commonly observed on the abyssal seafloor in many regions of the world ocean (Beaulieu 2002). These amorphous clumps of organic matter usually originate in surface waters and settle through the water column, undergoing changes facilitated by sinking, coagulation, and disaggregation, combined with bacterial and zooplankton consumption, while settling to the seafloor (Lampitt 1992; Kiørboe and Thygesen 2001; Stemmann et al. 2004). The principal identifiable fraction of detrital aggregates on the seafloor comprises planktonic organisms or their exuviae, including diatoms, radiolarians, bacteria, and zooplankton fecal pellets (Beaulieu and Smith 1998; Beaulieu 2002). The adhesive matrix joining these components together has a mucous consistency and can originate as material ranging from diatom exudates (Alldredge and Gotschalk 1989; Alldredge et al. 1993) to appendicularian feeding structures (Silver et al. 1998; Robison et al. 2005). The importance of these aggregates and the relationship of their presence to the rain of smaller sinking particulate matter generally collected in sediment traps have long been debated. Much of the larger material constituting detrital aggregates is believed to be undersampled by sediment traps and represents an often-ignored food supply to the deep-sea benthic community (Baldwin et al. 1998; Shaw et al. 1998; Robison et al. 2005). Detrital aggregates may contribute importantly to seafloor communities. Indeed, epibenthic megafauna spend more time in limited areas of the seafloor when detrital aggregates are present (Kaufmann and Smith 1997); individual megafauna have been observed associated with detrital aggregates (Lauerman and Kaufmann 1998); and sediment community oxygen consumption (SCOC) in cores containing detrital aggregates was significantly higher than in cores without aggregates (Smith et al. 1998).

Regional- and basin-scale climate indices have been correlated with sinking POC flux at abyssal depths in the NE Pacific (Smith et al. 2006). Here we examine the input of detrital aggregates combined with POC flux to the deep ocean and compare the timing and magnitude of this total food supply to upper-ocean processes. We test the null hypothesis that detrital aggregate density and size are not significantly related to POC flux entering the benthic boundary layer and to upper-ocean processes, reflected in such measures as climate indices, net primary production, and zooplankton displacement volume.

Methods

A time-lapse camera was deployed on the seafloor at an abyssal site (Sta. M) in the NE Pacific over a period of 17 yr, with seasonal servicing from 24 February 1990 until 24 March 2006. Sta. M is a long time-series station located on the Monterey Deep-Sea Fan at a depth of approximately 4100 m (Fig. 1). This abyssal station is characterized by a seasonal and interannually fluctuating food supply of particulate organic matter sinking to the seafloor, which has been correlated with climate variation, surface water production, and export flux (Smith et al. 2006). Oxygenated silty-clay sediments are distributed over the bottom with low topographic relief (Smith et al. 1994; Smith and Druffel 1998), and there are slow bottom boundary currents (2.19 ± 1.76 cm s^{-1} at 2.5 m above bottom) (Beaulieu and Baldwin 1998).

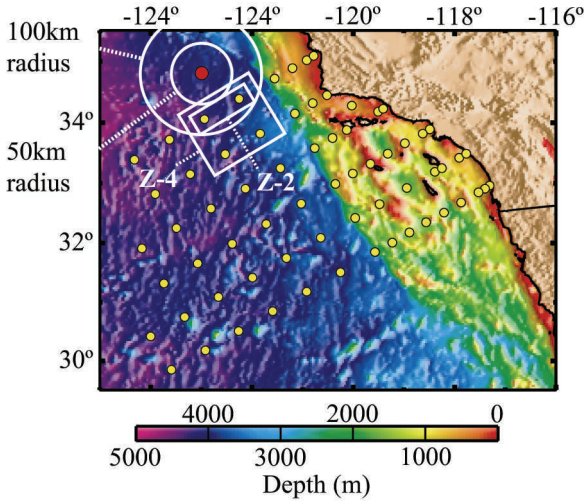

Fig. 1. Satellite-derived image of primary production along the southern California coast with Sta. M (red circle) shown in the upper left corner. Color differentiation indicates water depth. The 50- and 100-km–radius catchment areas around Sta. M (white circles) were used to estimate satellite-derived SST, Chl *a*, NPP, and export. The CalCOFI zooplankton sampling station grid (yellow circles) is shown to the south, with two blocks of stations used to estimate zooplankton displacement volume for two (Z-2) and four (Z-4) stations in proximity to Sta. M.

The long time-series mooring was established at Sta. M in June 1989 and since has been maintained seasonally with episodic lapses. This mooring has had two sediment traps, one each at 600 and 50 m above bottom (mab), with sequencing cups providing 10-d sampling resolution (Baldwin et al. 1998). Flotation was distributed along the mooring line to maintain tautness while not interfering with the sediment-trap collection efficiency. At the bottom of the mooring were a time-lapse camera system as well as the mooring acoustic releases and ballast. Sediment trap samples were prepared and processed following the procedures described by Baldwin et al. (1998).

The time-lapse camera consisted of a film camera (Fuji, type 8514, 500 ASA color negative film) mounted in the apex of a titanium frame with a 200 W-s and 400 W-s strobe positioned on lateral struts to either side of the camera to maximize seafloor illumination while reducing common-volume scattering (Smith et al. 1993). A 20-m^2 area of the seafloor was illuminated by the strobes, and an oblique photograph with a 50° horizontal angular view was taken every hour during each 3–4-month deployment.

Each oblique photograph was projected onto an acoustic digitizing pad overlaid with a perspective grid (Wakefield and Genin 1987). The position and areal coverage of each distinguishable detrital aggregate then was determined and calculated using an electronic digitizer interfaced with a computer. The radial distance of each aggregate was computed from the bottom center of each image. Using point transect theory (Buckland et al. 1993), a probability density function then was fitted to the observed distribution

of distances for each deployment (DISTANCE program; Laake et al. 1994). The visible area of the seafloor over which detrital aggregates could be detected depended on variations in strobe intensity and film processing as well as aggregate size and color in contrast to the surrounding sediment. The effective radius viewed during each deployment was determined by accounting for the probability of observing aggregates at various distances from the camera (Buckland et al. 1993). The effective viewed area for each deployment was calculated by accounting for the effective viewed radius from the camera origin and the horizontal angular view. Aggregate density, percent cover, and mean aggregate size were calculated on a daily and monthly basis for each deployment. The effective area of seafloor viewed was typically $\sim$5 m^2 for the aggregates over the course of the study period.

The detrital aggregate analyses used in this study differ from previous studies at Sta. M in the 1990–1991 and 1994–1995 study periods, when aggregate data were recorded every 4 h (Smith et al. 1994, 1998). Here, aggregate data were determined once every 24 h during each of the 27 camera deployments from 1990 to 2006 to obtain equivalent sampling effort throughout the entire study.

Satellite imaging of the surface ocean in the immediate vicinity of Sta. M provides valuable insights into surface conditions affecting primary production, the principal source of food supply to the abyssal benthic community. To estimate the surface conditions over Sta. M that would best represent the catchment area (statistical funnel; Siegel and Deuser 1997; Siegel and Armstrong 2002) for the abyssal sediment traps, we used 50- and 100-km–radius circles with the center over Sta. M. Our past calculations revealed a best statistical correlation between surface conditions within a 50- to 100-km–radius circle around Sta. M and POC flux at 50 mab (Smith et al. 2006). Satellite ocean color data, only available from 1996 to the present, were used to estimate net primary production and export flux from the euphotic zone. Chlorophyll *a* (Chl *a*) concentration was estimated from the ocean color and temperature scanner and the sea-viewing wide field-of-view sensor (SeaWiFS) monthly data for the two catchment areas around Sta. M. Net primary production (NPP) then was estimated using the carbon-based production model (CbPM; Behrenfeld et al. 2005). This model estimates NPP from satellite-derived chlorophyll : carbon ratios using a semianalytical approach (Maritorena et al. 2002). Export flux from the euphotic zone was calculated with a parameterization of Laws (2004) using NPP estimated from the CbPM and sea surface temperature (SST).

Long time-series collections of zooplankton in the upper 210 m of the water column have been conducted in the general region of Sta. M by the California Cooperative Oceanic Fisheries Investigations (CalCOFI) and California Current Ecosystem long-term ecological research programs (Ohman and Venrick 2003). Plankton tows were conducted using 0.505-mm mesh bongo nets with a 0.71-m–diameter opening (Ohman and Smith 1995). We chose seasonal measurements of total zooplankton displacement volume (DV), an estimate of biomass, using two station configurations, one with two stations within 100 km of Sta. M (Z-2) and one including two additional nearby stations (Z-4; Fig. 1).

Spearman rank cross-correlations (r; Zar 1998) were calculated to identify the intensity and timing of relationships between detrital aggregates on the seafloor, POC flux, upper water-column conditions, and climate indices. Probability values for the resulting correlation coefficients were corrected for serial autocorrelation where applicable, using methods described by Pyper and Peterman (1998).

Results

Seafloor detrital aggregates—There was a striking seasonal pattern of discrete detrital aggregates reaching the seafloor during the 17-yr monitoring period (Fig. 2). Detrital aggregates first became visible on the seafloor as early as June and continued to settle in subsequent pulses through the end of December, with a residual number occasionally visible into January. Over the time series, seasonal maxima in aggregate density were most frequently in September and October. Interannual variation in aggregate density was also high, with large peaks in 1990, 1994, 2001, and 2002 (Fig. 2a). Aggregate density reached the highest peaks of 23 m^{-2} in September and November 2001, the year during which the greatest number of aggregates was observed on the seafloor. Similarly high densities of aggregate settlement were apparent in two other years, 1994 and 2002. Years with the lowest aggregate densities were 1993, 1995, 1998, and 2004. The mean daily density over the 17-yr period was 1.82 $\pm$ 3.42 m^{-2} over a total of 2767 d of observation.

Sizes of individual detrital aggregates ranged from 0.3 cm^2 on 05 July 2001 to 1908.5 cm^2 on 23 October 1994. Of the 15,816 aggregates measured in this study, the peak in size distribution was shifted toward smaller sizes with a mode of 9 cm^2 (Fig. 3). Over 50% of the aggregates were smaller than 20 cm^2, and 95% were smaller than 115 cm^2. Peaks in daily mean aggregate size lagged the peaks of aggregate density during the two major aggregate sedimentation periods in November 1994 and August 2002 (Fig. 2b). Over the entire time series, detrital aggregate density was correlated significantly with mean aggregate size ($p < 0.001$, $r = 0.46$, $n = 1241$).

The percentage of the seafloor covered daily by detrital aggregates generally followed seasonal fluctuations in aggregate density (Fig. 2c). Daily mean aggregate density was highly correlated with aggregate percent cover throughout the time series, with no temporal lag ($p < 0.001$, $r = 0.99$, $n = 2767$). Daily mean aggregate size also was correlated with aggregate percent cover ($p < 0.001$, $r = 0.77$, $n = 1241$). However, during one period in August 2002, the percent aggregate cover increased dramatically, while aggregate density decreased, indicating the accumulation of larger aggregates but fewer numbers. Aggregate cover was generally <5% during most years but exceeded this value in 1994, 2001, 2002, and 2003. The highest percent coverage was 14.75% in August 2002 and 13.8% in November 1994, the 2 months with the highest sustained aggregate coverage (Fig. 2c).

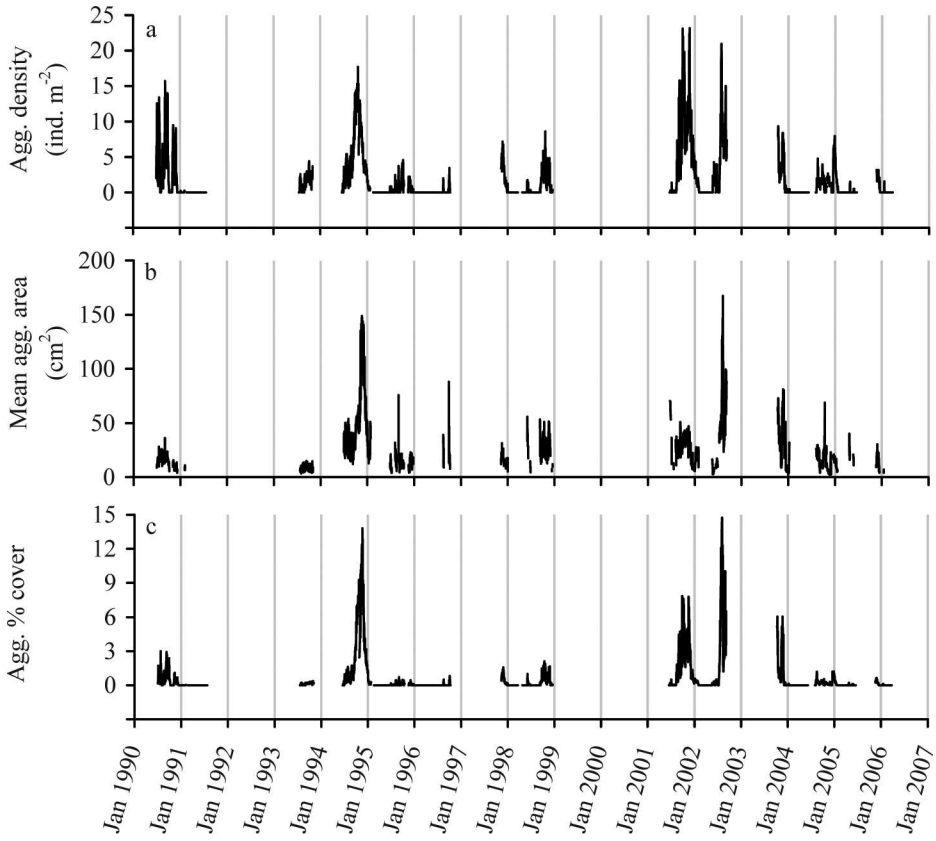

Fig. 2. Detrital aggregate (a) density, (b) mean aggregate size, and (c) percent seafloor cover measured daily at Sta. M from 23 February 1990 through 15 August 2006.

Abyssal water-column particulate matter flux—The primary source of the detrital aggregates is the sinking particulate matter entering from the overlying water column. Total mass flux and the component fractions of $CaCO_3$, total nitrogen, and POC exhibited considerable seasonal and interannual variation at 50 mab from 1990 through 2006 (Fig. 4). Particulate matter flux and each component fraction were correlated significantly with daily detrital aggregate density, as exemplified by total mass flux ($p < 0.001$, $r = 0.42$, $n = 2702$) and POC flux ($p < 0.001$, $r = 0.45$, $n = 2681$). Cross-correlations on a daily basis revealed no apparent time lag between fluctuations in particulate matter fluxes at 50 mab and aggregate density on the seafloor, indicating a coupling between these processes. Similarly, the cross-correlations between aggregate density and particulate matter fluxes at 600 mab, including total mass ($p < 0.001$, $r = 0.29$, $n = 1791$) and organic carbon fluxes ($p < 0.001$, $r = 0.35$, $n = 1781$), revealed no lag between the collection of pelagic flux and settlement on the seafloor. As expected from previous studies (Smith et al. 2006), there was no significant time lag between the particulate matter fluxes at 600 and 50 mab.

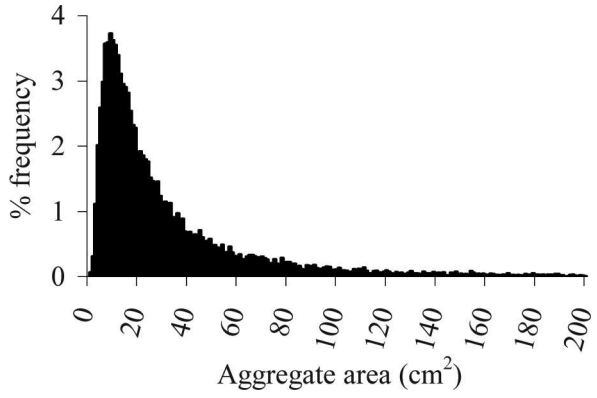

Fig. 3. Size–frequency distribution of individual detrital aggregates ($n = 15{,}816$) measured every 24 h over the entire monitoring period from 23 February 1990 through 15 August 2006. The upper tail of the distribution curve extending to 1908.5 cm^2 is cropped at 200 cm^2.

Daily detrital aggregate percent cover was significantly correlated ($p < 0.01$) with total mass flux and the three measured fractions at both 50 and 600 mab and, not surprisingly, showed the same temporal trends as the aggregate density comparisons above, with zero time lags (Fig. 4).

Upper water-column processes—The equatorward-flowing California Current is a prominent offshore feature in the surface waters above Sta. M, extending out from the more coastal Inshore Countercurrent that flows poleward (Bograd and Lynn 2003). Nutrient- and chlorophyll-enriched eddies generated from coastal upwelling filaments move offshore over Sta. M primarily in the spring and

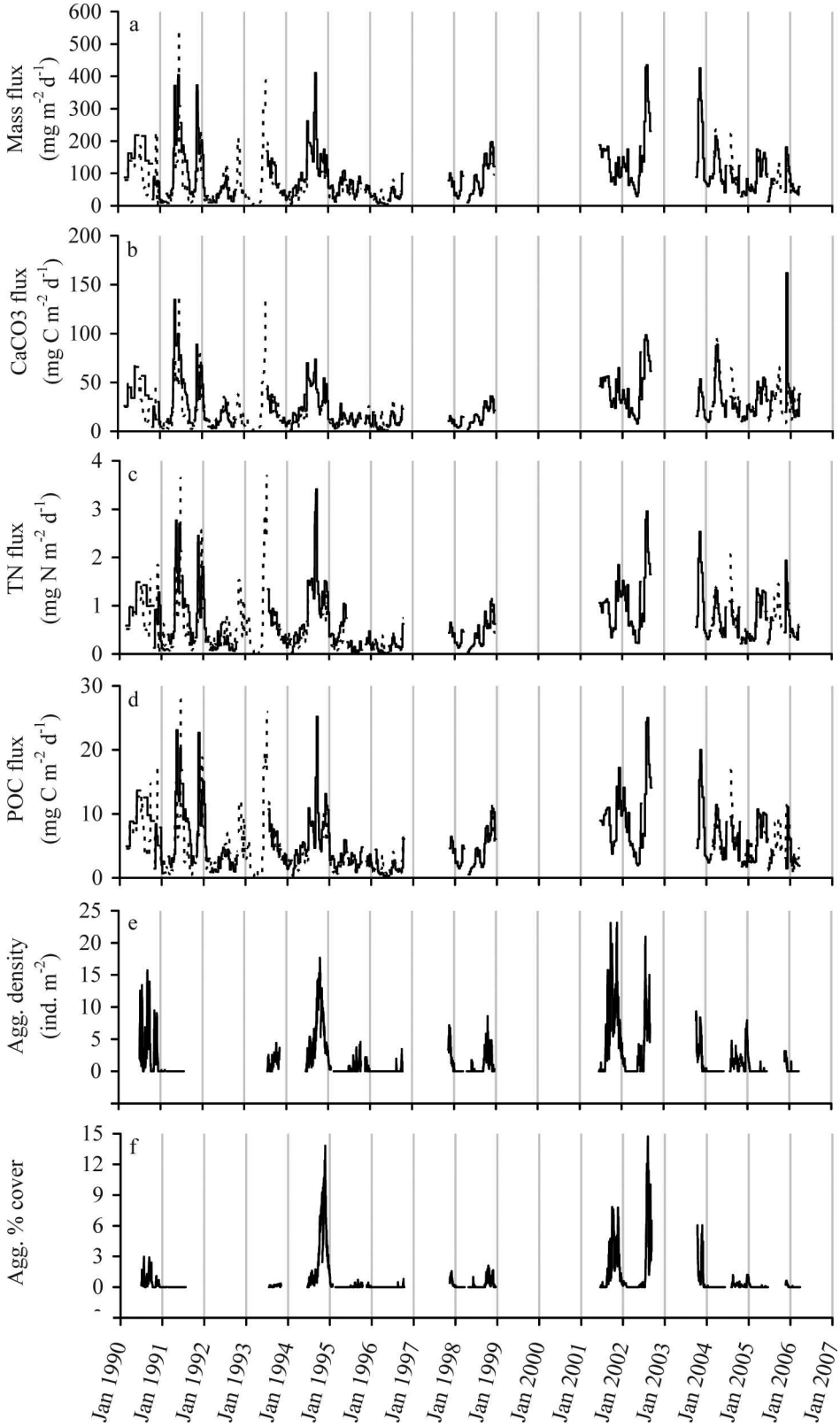

Fig. 4. Daily particulate matter flux at 50 mab (solid line) and 600 mab (dashed line), with detrital aggregate density and aggregate percent cover at Sta. M. Water-column measurements of (a) total mass flux and the following three components: (b) $CaCO_3$ flux, (c) total nitrogen flux, and (d) particulate organic carbon flux. Seafloor measurements of (e) detrital aggregate density and (f) detrital aggregate percent cover.

summer (fig. 1 in Smith et al. [2006]), but with considerable interannual variability.

In the area of Sta. M, satellite-estimated Chl *a* concentrations were low in 1998, corresponding to a major El Niño southern oscillation (ENSO) event (Kahru and Mitchell 2002), but were higher and relatively consistent from 1999 through early 2003, when fluctuations became greater in amplitude (Fig. 5b). The temporal pattern of the CbPM-based NPP was similar to that of Chl *a* (Fig. 5c). Detrital aggregate density averaged monthly over the time series from 1996 through 2006 was correlated significantly with the estimated export flux (EF), with a peak at a temporal lag of 3 months for both the 50-km–radius (Fig. 5d,e; $p = 0.03$, $n = 54$, $r = 0.44$) and 100-km–radius catchment circles (Fig. 5d,e; $p = 0.004$, $n = 54$, $r = 0.58$). A cross-correlation of aggregate percent cover and export flux also revealed a significant relationship for both catchment circles (100-km radius: $p < 0.001$, $n = 54$, $r = 0.54$; 50-km radius: $p = 0.002$, $n = 53$, $r = 0.41$), with a high in correlations after a lag of 3 months in each case. A peak lag of 3 months between export flux and the arrival of detrital aggregates on the seafloor seems reasonable, considering transport through the water column and possible repackaging, with adhesion and aggregation processes on the descent. Particle settling speeds range from <1 m d^{-1} for small algal cells to >100 m d^{-1} for fecal material and large marine snow (Stemmann et al. 2004). A settling speed of $\sim$40 m d^{-1} is reasonable, assuming a transit from the base of the euphotic zone to 4100 m in depth at Sta. M. Given the range of significance for cross-correlations between export flux and seafloor aggregate density of 1–4 months, aggregate sinking speeds are likely in the range of $\sim$34–137 m d^{-1}.

From phytoplankton, the next trophic link in the production of sinking particulate matter is the zooplankton. The mean displacement volume (DV) of total zooplankton for both CalCOFI station configurations (Z-2 and Z-4; Fig. 1) exhibited peaks in 1992 and 1996–1998. Amplitude of the seasonal peaks in DV decreased after 1999, following the proposed regime shift in 1998 (Bograd et al. 2000), but the overall mean zooplankton abundance was greater after 1998 than before. Net primary production, calculated using the CbPM model data, was significantly correlated with changes in zooplankton DV within both the Z-2 and Z-4 configurations for the 100-km–radius circle around Sta. M (Z-2: $p = 0.005$, $n = 36$, $r = 0.46$; Z-4: $p = 0.016$, $n = 37$, $r = 0.39$). The resulting EF was also significantly correlated with zooplankton DV (Z-2: $p < 0.006$, $n = 36$, $r = 0.45$; Z-4: $p < 0.004$, $n = 37$, $r = 0.46$). In the transition from surface water to abyssal depths, a significant cross-correlation relationship existed between zooplankton DV and POC flux (50 mab) with a $\leq$1-month lag (Fig. 6a,b; peak correlations: Z-2: $p = 0.005$; $n = 45$, $r = 0.41$; Z-4: $p = 0.020$, $n = 46$, $r = 0.34$). A similar $\leq$1-month lag was significant between zooplankton DV and detrital aggregate density on the seafloor (Fig. 6a,c; peak correlations: Z-2: $p = 0.057$; $n = 32$, $r = 0.34$; Z-4: $p = 0.028$, $n = 33$, $r = 0.38$).

Climate indices—We conducted time-series analysis of four climate indices critical to processes in the North Pacific: the oceanic-scale southern oscillation index (SOI) and multivariate ENSO index (Wolter and Timlin 1998), the basin-scale NOI (Schwing et al. 2002), and the regional-scale Bakun upwelling index (BUI; Bakun 1973). The time-lagged correlations between aggregate density and the SOI, MEI, and NOI were not significant ($p > 0.05$), but the sign and timing of the peaks were in agreement with the links between climate and POC flux previously reported at Sta. M (Smith et al. 2006; Fig. 7a–c,e). A more regional spatial scale comparison of the BUI with detrital aggregate density was highly significant with a lag of 3 months (Fig. 7d,e; $p < 0.001$, $n = 102$, $r = 0.75$).

Discussion

Correlations between detrital aggregate density and upper water-column processes indicate a strong pelagic to benthic coupling. We propose the following sequence of events between the surface and the seafloor. Spring peaks in upwelling intensity along the central California coast, reflected in a positive BUI, bring nutrient-rich water to the surface, stimulating phytoplankton growth. Phytoplankton growth, manifested as net primary production, leads to some export flux of particulate material out of the euphotic zone (Alldredge and Gotschalk 1989). Cross-correlation analyses indicated that these first events leading to the production of sinking particulate matter occur around 1–4 months prior to evidence of such events appearing at abyssal depths (Fig. 8a–c). Also, in the surface waters, zooplankton follow the enhanced level of primary production, with increased abundance within a month (Fig. 8d), contributing to trophically repackaged particulate matter, some portion of which sinks to the seafloor. There is a hiatus of $\leq$1 month between peaks in zooplankton DV (Z-4) and the following highs in particulate matter fluxes at 600 and 50 mab (3500 and 4050 m in depth) and detrital aggregate densities on the seafloor (Fig. 8d,e). Of course, correlations alone are not conclusive, especially where seasonal patterns exist. In addition to the timing and intensity of the cross-correlations, substantial contextual information was used to formulate our temporal scenario.

Timing of these events indicates that trophic repackaging of organic matter by the zooplankton contributes to detrital aggregates on the seafloor. The structural composition of the sinking particulate organic matter entering the benthic boundary layer and detrital aggregates on the seafloor at Sta. M have a high percentage of zooplankton fecal pellets and exuviae (Beaulieu and Smith 1998). Salp fecal material is very conspicuous in the abyssal sediment-trap samples from Sta. M and is most prevalent in the fall (K. Smith unpubl.) during peaks in detrital aggregate density on the seafloor (Fig. 2). Studies in other deep-sea regions also have shown a strong contribution of zooplankton to the flux of particulate organic matter to the deep-sea floor (Pfannkuche and Lochte 1993; Robison et al. 2005). However, this does not preclude the potential importance of phytodetritus reaching the seafloor without intervention by zooplankton (Beaulieu 2002).

Over the 17-yr time series there were several strong peaks in aggregate density on the seafloor, which corresponded to

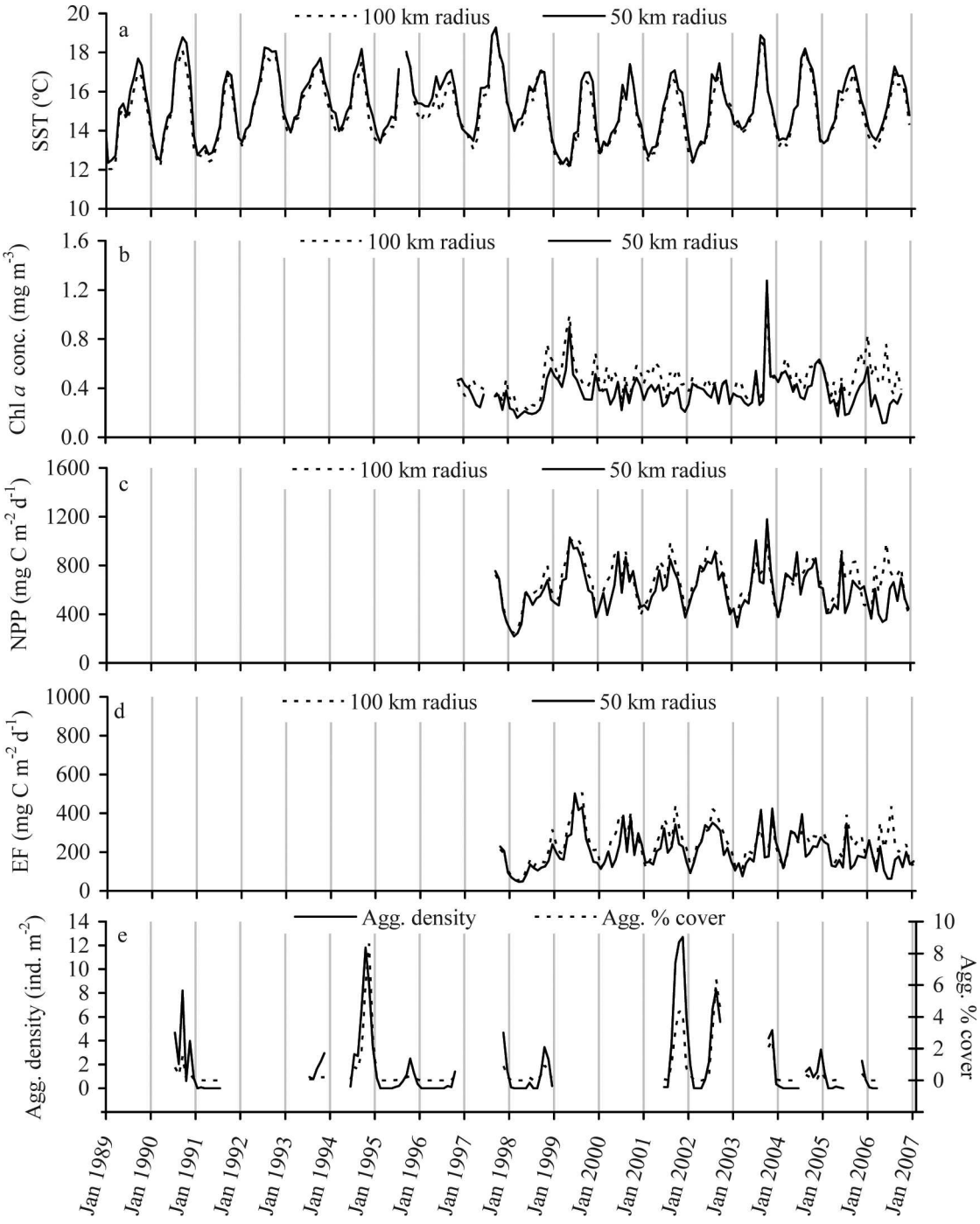

Fig. 5. Monthly averaged surface ocean conditions in 50-km– and 100-km–radius circles around Sta. M compared to detrital aggregate density and percent cover on seafloor. (a) Sea surface temperature (SST) from January 1989 through 2006. (b) Chlorophyll *a* (Chl *a*), (c) net primary production (NPP, calculated using the CbPM model), and (d) export flux (EF) over the period from 1997 through 2006. The 50-km– and 100-km–radius estimates of surface conditions are expressed as solid and dashed lines, respectively. (e) Seafloor measurements of detrital aggregate density (solid line) and aggregate percent cover (dashed line).

similar peaks in the mass and POC fluxes at 600 and 50 mab. It often has been shown that sediment traps can clog with large settling aggregates and that subsequent calculations of fluxes underestimate the real settlement rate of particulate matter to the seafloor (Baldwin et al. 1998; Beaulieu and Smith 1998). The coincidence of the peaks in POC flux and the density of aggregates on the seafloor support the idea that both settlement events are in synchrony, but is the total flux some combination of these measured fluxes? The total flux is certainly not the sum of both fluxes, since some portion of the detrital aggregates passes through the baffles of the sediment trap and

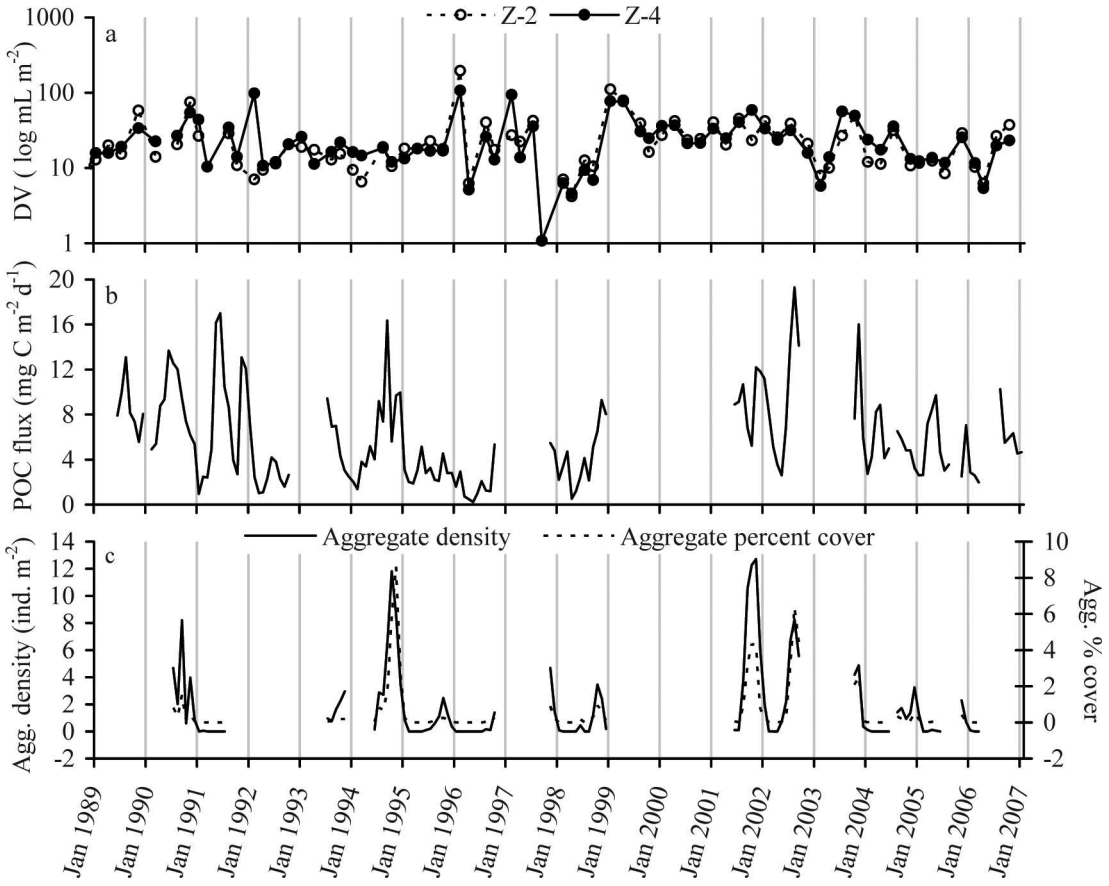

Fig. 6. Monthly zooplankton displacement volume compared to abyssal measurements of POC flux and detrital aggregate density and aggregate percent cover on the seafloor. (a) Zooplankton displacement volume (DV) was calculated for a two-station (Z-2, dashed line) and four-station (Z-4, solid line) configuration (*see* Fig. 1). (b) POC flux measured at 50 mab. (c) Seafloor measurements of detrital aggregate density (solid line) and aggregate percent cover (dashed line).

becomes part of the measured water-column flux. Openings in the baffle across the 0.25-m^2 mouth of the sediment trap are 1 cm^2. The size range of settled detrital aggregates in this study ranged from 0.3 to 1908.5 cm^2, with the frequency distribution shifted toward the smaller end of the size spectrum on the seafloor (Fig. 3). Clogging of sediment traps has been documented in several deep-sea studies (Baldwin et al. 1998). However, the extent to which such clogging events influence the estimates of particulate matter fluxes is largely unknown. Obviously, neither the traps nor the time-lapse camera monitoring of the seafloor gives a complete picture of flux rates. Smaller particles go undetected by the camera but are collected by the traps, while larger particles can escape detection by the traps but are observed by the camera.

Particles in the water column range in size from 1 μm to 1 cm in diameter (Stemmann et al. 2004). These smaller particles can then become aggregated into larger particles that we observe on the seafloor. Seafloor aggregates consist of planktonic organisms and exudates, including diatoms, radiolarians, bacteria, and zooplankton fecal pellets (Beaulieu and Smith 1998). Aggregation appears to be facilitated by a mucous matrix that can originate from a number of sources, ranging from diatom exudates (Alldredge and Gotschalk 1989; Alldredge et al. 1993) to appendicularian feeding structures (Silver et al. 1998; Robison et al. 2005).

A comparison can be made between the chemical composition of detrital aggregates and that of sinking particulate matter collected in the sediment traps. A large number of individual detrital aggregates were collected in Alvin tube cores at Sta. M during two dive series in August ($n = 52$) and September 1994 ($n = 79$) (Smith et al. 1998). The area of each aggregate was measured, the chemical composition analyzed, and a regression equation fitted to the data from each cruise. Using the regression equations for organic carbon composition from August and September as a range, we estimated the organic carbon content of each aggregate in our study from their individual measured areas. This calculation assumes that the detrital aggregates measured in this study have a comparable chemical composition to those measured in 1994.

The principal peaks in the standing stock of aggregate organic carbon occurred in the fall in 1994, 2001, and 2002, generally following peaks in POC flux at 50 mab (Fig. 9a). The highest peak of aggregate organic carbon in fall 1994 reached 161 mg C m^{-2}, compared with the concurrent POC flux of 9.7 mg C m^{-2} d^{-1}. Although the standing stock of aggregate carbon on the seafloor cannot be

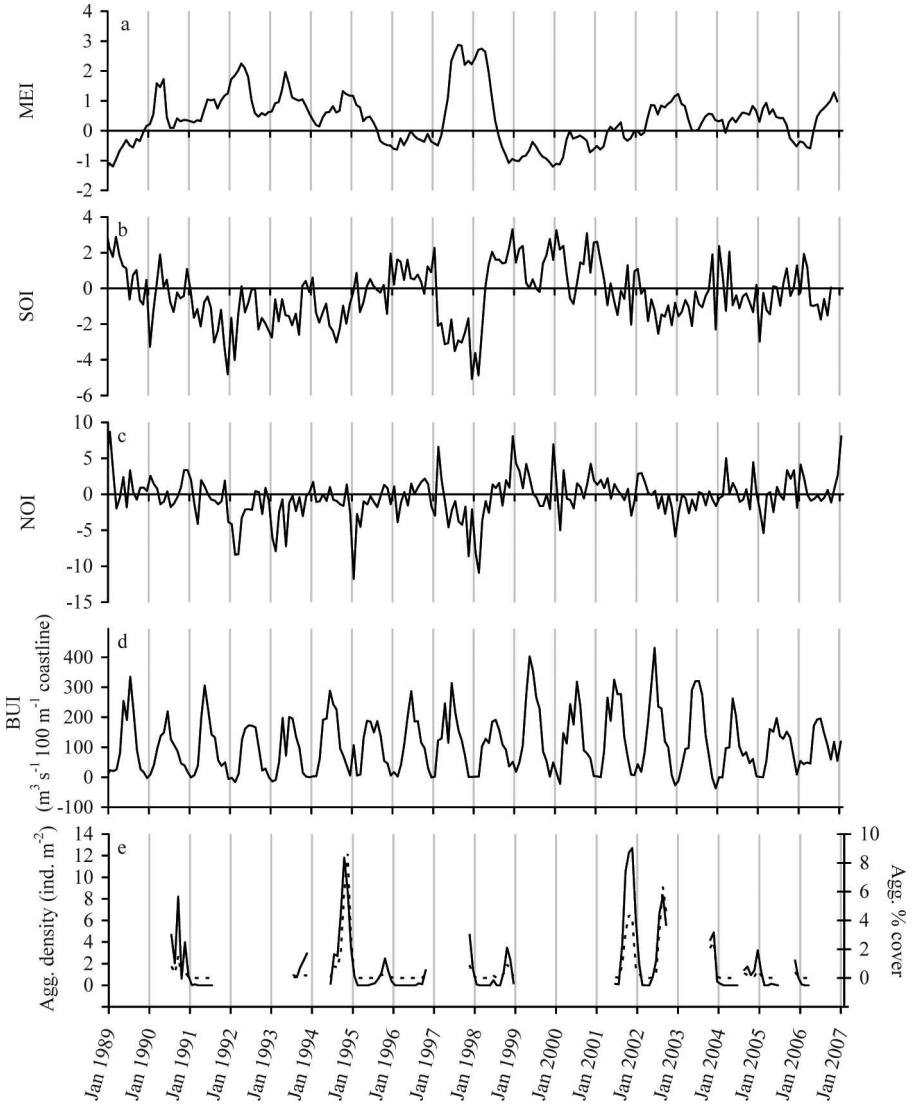

Fig. 7. A comparison of oceanic- and regional-scale climate indices with detrital aggregate density and percent cover on the seafloor from 1989 through 2006. (a) The basin-scale multivariate El Niño southern oscillation index (MEI), (b) southern oscillation index (SOI), and (c) northern oscillation index (NOI). (d) The regional-scale Bakun upwelling index (BUI). (e) Seafloor measurements of detrital aggregate density (solid line) and aggregate percent cover (dashed line).

directly compared with the flux of POC, the substantial peaks in aggregate material certainly exhibit seasonal and interannual pulses of food to the benthic community. This significant source of food to the benthos is readily available to the epibenthic megafauna (Lauerman et al. 1997) and the sediment community (Smith et al. 1998).

Previous studies showed that detrital aggregates have a visible residence time on the seafloor of 45–95 h at Sta. M (Smith et al. 1994, 1998). We calculated the rate of organic carbon input to the seafloor as aggregates by dividing the daily aggregate organic carbon standing stock by the previously estimated residence time (Fig. 9b). The higher aggregate organic carbon (AOC) flux limit represents the September 1994 estimate of aggregate organic carbon with a 45-h residence time, and the lower limit uses the August 1994 estimate of aggregate organic carbon with a 95-h residence time. Because the AOC flux estimates and aggregate percent cover are both based on aggregate area, they have the same variation but differing amplitudes. Thus, Spearman rank correlations between various parameters and AOC flux will be the same as with aggregate percent cover. For 24% of the days for which both aggregate images and POC flux data were available, estimated AOC flux was greater than the concurrently measured POC flux for the higher estimate and 6% for the lower flux estimate (Fig. 9c). Periods of high detrital aggregate input were particularly prevalent in 1994, 2001, and 2002. The lower AOC flux estimate only exceeded POC flux during autumn periods in 1994 and 2001. Using the upper and lower estimates of organic carbon flux, we

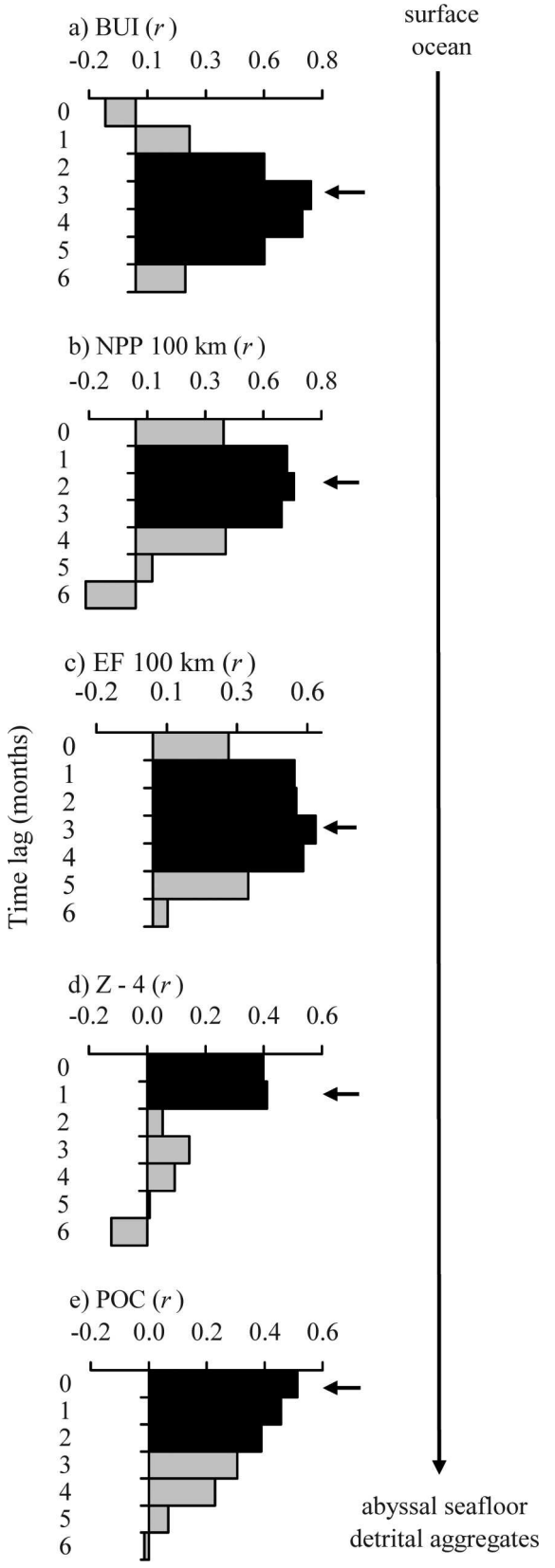

Fig. 8. Spearman rank cross-correlations (r) of monthly regional surface ocean conditions and abyssal POC flux, all lagged at monthly intervals on the vertical axis, to detrital aggregate density on the seafloor. Correlations with $p \leq 0.05$ are in black, and correlations with $p > 0.05$ are shaded gray, illustrating the temporal range of significance. Arrows delineate the peaks in cross-correlations. (a) Bakun upwelling index (BUI). (b) Net primary production (NPP) calculated for 100-km–radius circle around Sta. M. (c) Export flux (EF) calculated for 100-km–radius circle around Sta. M. (d) Zooplankton displacement volume (DV) estimated for the four-station configuration (Z-4). (e) POC flux measured at 50 mab.

calculated a ratio of AOC flux to POC flux (Fig. 9c). The AOC flux : POC flux estimates indicate that detrital aggregates at higher fluxes can constitute an important input of food to the deep-sea benthos and in some combination with POC flux should yield a higher rate of food supply to the benthic community than previously thought when treating POC flux as the only food source (Smith and Kaufmann 1999). As we argued above, it is impossible to separate the aggregate and POC flux inputs, since some portion of the aggregate accumulation also should be collected by sediment traps. However, the higher input rate of detrital aggregates compared to concurrently measured POC flux at certain times argues that some portion of the particulate matter escapes detection in the sediment traps. Even if aggregate fluxes do not exceed trap-measured POC fluxes most of the time, the detrital aggregate organic carbon input reaching the seafloor on a daily basis can be as high as 378–514% more than the POC flux, as on 20 November 1994 and 27 September 2001, respectively.

Particulate matter trapping efficiency was measured previously using estimates of radionuclide accumulation from the sediment trap at 50 mab at Sta. M concurrently with measurements from detrital aggregates collected from the seafloor. Shaw et al. (1998) found that the sediment trap–determined flux of ex^{210}Pb and ex^{230}Th significantly underestimated water-column production by almost an order of magnitude. Shaw and associates were able to reconcile this discrepancy with the additional delivery of ex^{230}Th as large detrital aggregates at Sta. M.

A discrepancy between the food supply entering the deep sea and the food demand by the sediment community at Sta. M has been well documented. A ratio of the food supply, as POC flux entering the benthic boundary layer, and the food demand, as SCOC, decreased steadily from a high of 0.99 in 1989–1990 to 0.22 in 1995–1996 (Smith and Kaufmann 1999). Afterwards, there was an increase in POC flux : SCOC up to 0.43 in 1998 based on increased POC flux (Smith et al. 2001). Other sources of food supply exist, such as the organic carbon already incorporated in the sediments and that introduced by lateral transport along the continental margin (Smith et al. 2001). Another source is the detrital aggregates that cannot be totally accounted for by the POC flux measurements made with sediment traps. Unfortunately, there was a long hiatus in SCOC measurements from the end of 1998 until 2005. However, the monthly estimates of POC flux : SCOC through the observational period still show an insufficient food supply to meet the demand overall (Fig. 9d). Of those

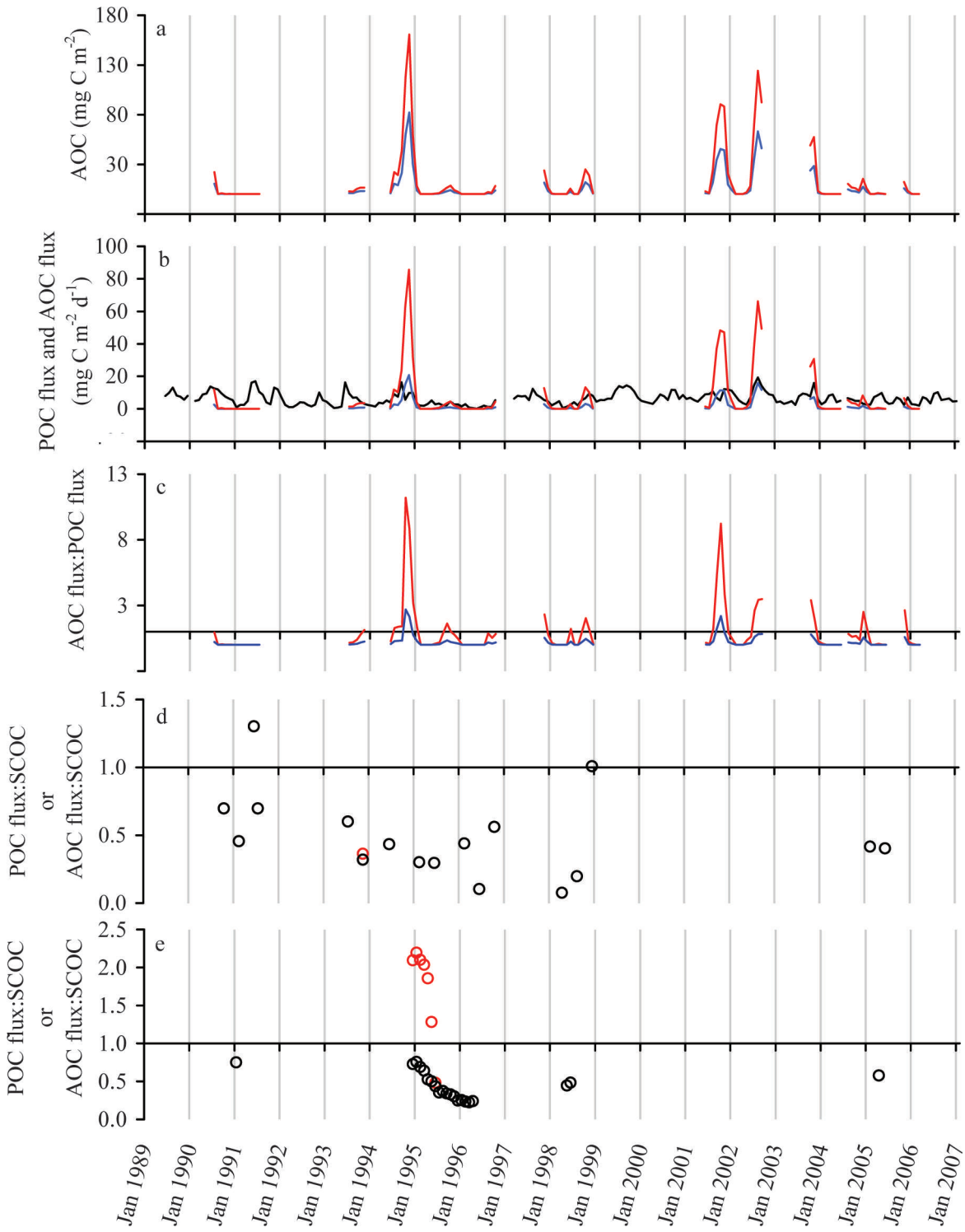

Fig. 9. Estimated organic carbon content of the detrital aggregates and flux at Sta. M compared to the abyssal particulate organic carbon (POC) flux, detrital aggregate organic carbon (AOC) flux : POC flux, and maximum POC flux : sediment community oxygen consumption (SCOC) from 1989 to 2007. (a) Detrital AOC estimated from the August 1994 aggregate size to organic carbon regression (low values, blue line) and from the September 1994 aggregate size to organic carbon regression (high values, red line); *see* Smith et al. (1998) for regression equations. (b) AOC flux estimated using a residence time of 45 h (high flux rates, red line) and a residence time of 95 h (lower flux rates, blue line) compared to the POC flux as a composite measurement between 50 and 600 mab (black line). (c) The ratio of AOC flux to POC flux for both the low-rate (blue line) and high-rate (red line) estimates. The horizontal black line indicates a ratio of 1 to 1. (d) The ratio of the POC flux (either POC flux or AOC flux, whichever value is higher) to concurrently measured SCOC on a monthly basis (black open circles). November 1993 (red open circle) was the only month during which AOC flux exceeded the measured POC flux and during which there was a concurrent SCOC measurement. (e) A 13-month centered running mean of the ratio of POC flux to SCOC using either POC flux (black open circles) or AOC flux (red open circles) as in (d). Horizontal black line indicates a ratio of 1 to 1.

periods during which sedimentation-trap, visual aggregate, and SCOC data are synoptic, there was only one monthly period in November 1993 during which the detrital AOC flux was higher than the POC flux, with a resulting ratio that still measured less than 0.5 (Fig. 9d). POC flux only exceeded SCOC in June 1991 and December 1998. Over 13-month periods during which POC flux, SCOC, and AOC flux were available, the AOC flux : SCOC ratio substantially exceeded unity (2.1) from December 1994 to May 1995, but only using the higher organic carbon estimates (Fig. 9e). Although there are considerable gaps in the data sets, it is still apparent that detrital aggregates occasionally can constitute substantial organic carbon inputs to the benthos and should be considered in estimates of food supply to deep-sea communities. Such detrital aggregate inputs are episodic and significantly correlated with surface ocean processes. The correlation of surface ocean processes, including climate, phytoplankton production, and zooplankton biomass, to abyssal benthic processes strongly reflects the functional complexity of the open-ocean ecosystem, especially in relation to the transport and processing of organic material. The marine carbon cycle can only be resolved with full ocean depth studies from surface to the seafloor over adequate temporal scales to capture the variability of marine systems.

References

Alldredge, A. L., and C. C. Gotschalk. 1989. Direct observations of the mass flocculation of diatom blooms: Characteristics, settling velocities and formation of diatom aggregates. Deep-Sea Res. **36:** 159–171.

———, U. Passow, and B. E. Logan. 1993. The abundance and significance of a class of large, transparent organic particles in the ocean. Deep-Sea Res. I **40:** 1131–1140.

Bakun, A. 1973. Coastal upwelling indices, west coast of North America, 1946–1971. NOAA Technical Report NMFS SSRF-671. U.S. Department of Commerce.

Baldwin, R. J., R. C. Glatts, and K. L. Smith, Jr. 1998. Particulate matter fluxes into the benthic boundary layer at a long time-series station in the abyssal NE Pacific: Composition and fluxes. Deep-Sea Res. II **45:** 643–666.

Beaulieu, S., and R. Baldwin. 1998. Temporal variability in currents and the benthic boundary layer at an abyssal station off central California. Deep-Sea Res. II **45:** 587–615.

Beaulieu, S. E. 2002. Accumulation and fate of phytodetritus on the sea floor. Oceanogr. Mar. Biol. Ann. Rev. **40:** 171–232.

———, and K. L. Smith, Jr. 1998. Phytodetritus entering the benthic boundary layer and aggregated on the sea floor in the abyssal NE Pacific: Macro- and microscopic composition. Deep-Sea Res. II **45:** 781–815.

Behrenfeld, M. J., E. Boss, D. A. Siegel, and D. M. Shea. 2005. Carbon-based ocean productivity and phytoplankton physiology from space. Glob. Biogeochem. Cycles **19:** GB1006, doi:10.1029/2004GB002299.

———, and others. 2006. Climate-driven trends in contemporary ocean productivity. Nature **444:** 752–755.

Bograd, S. J., and R. J. Lynn. 2003. Long-term variability in the Southern California Current System. Deep-Sea Res. I **50:** 2355–2370.

———, and others. 2000. The state of the California Current, 1999–2000: Forward to a new regime? Calif. Cooperative Oceanic Fish. Investig. Rep. **41:** 26–52.

Bopp, L., O. Aumont, P. Cadule, S. Alvain, and M. Gehlen. 2005. Response of diatoms distribution to global warming and potential implications: A global model study. Geophys. Res. Lett. **32:** L19606, doi:10.1029/2005GL023653.

Buckland, S. T., D. R. Anderson, K. P. Burham, and J. L. Laake. 1993. Distance sampling: Estimating abundance of biological populations.. Chapman & Hall.

Buesseler, K. O., and others. 2007. Revisiting carbon flux through the ocean's twilight zone. Science **316:** 567–570.

Kahru, M., and B. G. Mitchell. 2002. Influence of the El Niño–La Niña cycle on satellite-derived primary production in the California Current. Geophys. Res. Lett. **29:** 1846.

Kaufmann, R. S., and K. L. Smith, Jr. 1997. Activity patterns of mobile epibenthic megafauna at an abyssal site in the eastern North Pacific: Results from a 17-month time-lapse photographic study. Deep-Sea Res. I **44:** 559–579.

Kiørboe, T., and U. H. Thygesen. 2001. Fluid motion and solute distribution around sinking aggregates. II. Implications for remote detection by colonizing zooplankters. Mar. Ecol. Prog. Ser. **211:** 15–25.

Laake, J. L., S. T. Buckland, D. R. Anderson, and K. P. Burnham. 1994. DISTANCE Users Guide, V. 2.1. Colorado Cooperative Fish and Wildlife Research Unit, Colorado State Univ.

Lampitt, R. S. 1992. The contribution of deep-sea macrozooplankton to organic remineralization: Results from sediment trap and zooplankton studies over the Madeira Abyssal Plain. Deep-Sea Res. **39:** 221–233.

Lauerman, L. M. L., and R. S. Kaufmann. 1998. Deep-sea epibenthic echinoderms and a temporally varying food supply: Results from a one year time series in the N.E. Pacific. Deep-Sea Res. II **45:** 817–842.

———, J. M. Smoak, T. J. Shaw, W. S. Moore, and K. L. Smith, Jr. 1997. ^{234}Th and ^{210}Pb evidence for rapid ingestion of settling particles by mobile epibenthic megafauna in the abyssal NE Pacific. Limnol. Oceanogr. **42:** 589–595.

Laws, E. A. 2004. Export flux and stability as regulators of community composition in pelagic marine biological communities: Implications for regime shifts. Prog. Oceanogr. **60:** 343–354.

Maritorena, S., D. A. Siegel, and A. R. Peterson. 2002. Optimization of a semianalytical ocean color model for global-scale applications. Appl. Opt. **41:** 2705–2714.

Ohman, M. D., and P. E. Smith. 1995. A comparison of zooplankton sampling methods in the CalCOFI time series. Calif. Cooperative Oceanic Fish. Investig. Rep. **36:** 153–158.

———, and E. Venrick. 2003. CalCOFI in a changing ocean. Oceanography **16:** 76–86.

Pfannkuche, O., and K. Lochte. 1993. Open ocean pelago-benthic coupling: Cyanobacteria as tracers of sedimenting salp feces. Deep-Sea Res. **40:** 727–737.

Pyper, B. J., and R. M. Peterman. 1998. Comparison of methods to account for autocorrelation in correlation analyses of fish data. Can. J. Fish. Aquat. Sci. **55:** 2127–2140.

Robison, B. H., K. R. Reisenbichler, and R. E. Sherlock. 2005. Giant larvacean houses: Rapid carbon transport to the deep sea floor. Science **308:** 1609–1611.

Schwing, F. B., T. Murphree, and P. M. Green. 2002. The northern oscillation index (NOI): A new climate index for the northeast Pacific. Prog. Oceanogr. **53:** 115–139.

Shaw, T. J., J. M. Smoak, and L. Lauerman. 1998. Scavenging of ex^{234}Th, ex^{230}Th, and ex^{210}Pb by particulate matter in the water column of the California continental margin. Deep-Sea Res. II **45:** 763–779.

SIEGEL, D. A., AND R. A. ARMSTRONG. 2002. Corrigendum to "Trajectories of sinking particles in the Sargasso Sea: modeling of statistical funnels above deep-ocean sediment traps" [Deep-Sea Research I **44:** 1519–1541]. Deep-Sea Res. I **49:** 1115–1116.

———, AND W. G. DEUSER. 1997. Trajectories of sinking particles in the Sargasso Sea: Modeling of statistical funnels above deep ocean sediment traps. Deep-Sea Res. I **44:** 1519–1541.

SILVER, M. W., S. L. COALE, C. H. PILSKALN, AND D. R. STEINBERG. 1998. Giant aggregates: Importance as microbial centers and agents of material flux in the mesopelagic zone. Limnol. Oceanogr. **43:** 498–507.

SMITH, K. L., JR., R. J. BALDWIN, R. C. GLATTS, AND R. S. KAUFMANN. 1998. Detrital aggregates on the sea floor: Chemical composition and aerobic decomposition rates at a time-series station in the abyssal NE Pacific. Deep-Sea Res. II **45:** 843–880.

———, ———, H. A. RUHL, M. KAHRU, B. G. MITCHELL, AND R. S. KAUFMANN. 2006. Climate effect on food supply to depths greater than 4,000 meters in the northeast Pacific. Limnol. Oceanogr. **51:** 166–176.

———, AND E. R. M. DRUFFEL. 1998. Long time-series studies of the benthic boundary layer at an abyssal station in the NE Pacific. Deep-Sea Res. II **45:** 573–586.

———, AND R. S. KAUFMANN. 1999. Long-term discrepancy between food supply and demand in the deep eastern North Pacific. Science **284:** 1174–1177.

———, ———, AND R. J. BALDWIN. 1994. Coupling of near-bottom pelagic and benthic processes at abyssal depths in the eastern North Pacific Ocean. Limnol. Oceanogr. **39:** 1101–1118.

———, ———, ———, AND A. F. CARLUCCI. 2001. Pelagic-benthic coupling in the abyssal eastern North Pacific: An 8-year time-series study of food supply and demand. Limnol. Oceanogr. **46:** 543–556.

———, ———, AND W. W. WAKEFIELD. 1993. Mobile megafaunal activity monitored with a time-lapse camera in the abyssal North Pacific. Deep-Sea Res. I **40:** 2307–2324.

STEMMANN, L., G. A. JACKSON, AND D. IANSON. 2004. A vertical model of particle size distributions and fluxes in the midwater column that includes biological and physical processes. Part I: Model formulation. Deep-Sea Res. I **51:** 865–884.

WAKEFIELD, W. W., AND A. GENIN. 1987. The use of the Canadian (perspective) grid in deep-sea photography. Deep-Sea Res. **34:** 469–478.

WOLTER, K., AND M. S. TIMLIN. 1998. Measuring the strength of ENSO events: How does 1997/98 rank? Weather **53:** 315–324.

ZAR, J. H. 1998. Biostatistical analysis, 4th ed. Prentice Hall.

Received: 1 February 2008
Accepted: 21 June 2008
Amended: 8 August 2008